

Neutrino Physics: an Introduction

Amol Dighe

Tata Institute of Fundamental Research

Abstract

These are the lecture notes of the Neutrino Physics course at the SERC school in IIT Kanpur in Dec 2004. It is intended to be a first course in neutrinos, introducing the students to the phenomenology of neutrino masses, mixings and oscillations. It also discusses neutrino mass generation, the connection of neutrinos with astrophysics and cosmology, and reviews the current and future experiments related to neutrinos.

1 Organization of the lecture notes

The lectures start with Sec. 2 giving a historical perspective on neutrinos and their role in the SM even before the current excitement regarding their masses and mixing started. Neutrino oscillations in vacuum are introduced in Sec. 3 through the atmospheric neutrino problem and its resolution. Propagation of neutrinos through matter and its effect on their masses and mixings is explored in Sec. 4, for constant as well as varying matter densities. This is used in the resolution of the solar neutrino problem in Sec. 5. A consistent three neutrino framework that incorporates the solutions to the solar and atmospheric neutrino anomalies is introduced in Sec. 6.

Sec. 7 discusses the issues related to Dirac vs. Majorana nature of neutrinos and CP violation. Sec. 8 comments on the neutrino mass models that try to give rise to the observed mass and mixing spectrum. Sec. 9 points out some astrophysical and cosmological scenarios where neutrinos play an important role. Sec. 10 lists some of the current and future experiments whose results will further enhance our knowledge of neutrinos.

I have borrowed heavily from the “textbooks” [1, 2] and a review [3]. Since the notes are supposed to be pedagogical, the references are not necessarily where the concepts were first introduced, but where they are explained in detail.

2 Neutrinos in the SM : Massless neutrinos

In this section, we shall trace the history of neutrinos: their discovery and the role they have played in our understanding of the standard model (SM), even before they were found to have mass.

2.1 The first evidence for neutrinos

For two-body decays, the energy of each of the decay products in the rest frame of the decaying particle is a fixed quantity. Therefore, the observation of continuous electron energy spectra for beta decays of nuclei, where only the daughter nucleus and the emitted electron were observed, posed a puzzle. Either the conservation of energy and momentum was in peril, or something was missing. Pauli proposed (1932) that this missing something is a chargeless and massless particle, termed “neutrino”.

The introduction of such a particle not only took care of the energy-momentum conservation, it also explained the shape of the electron spectrum observed. Indeed, when the beta decay is a three-body decay, the decay rate is

$$\frac{d\Gamma}{dE_e} \propto p_e E_e (E_0 - E_e) \sqrt{(E_0 - E_e)^2 - m_\nu^2} \quad , \quad (1)$$

where p_e and E_e are the momentum and energy of the electron respectively, m_ν is the mass of the neutrino and $E_0 \equiv Q - m_e - m_\nu$ is the maximum energy of the electron.

When neutrino is massless, the slope of the “Kurie plot”

$$\frac{d\Gamma/dt}{p_e E_e} \propto \left[(E_0 - E_e) \sqrt{(E_0 - E_e)^2 - m_\nu^2} \right]^{1/2} \quad (2)$$

is a constant. The beta decay experiments till now have found the energy spectrum to be consistent with a massless neutrino, and have only been able to put an upper limit of 2.2 eV (95% C.L.) [4] on the mass of the “electron” neutrino. ¹

¹Since now we know that the electron neutrino is a superposition of three neutrino mass eigenstates, the mass measured in the beta decay experiments is actually a combination of the neutrino mass eigenvalues and mixing angles [2].

2.2 Discoveries of the three neutrino species

The first direct observation of neutrinos was by Reines and Cowan in 1956, wherein they directed a flux of $\bar{\nu}_e$ (supposed to have come from a beta decay) into a water target. The reaction $\bar{\nu}_e p \rightarrow n e^+$ produced positrons, which annihilated with electrons in the scintillation counters giving two 0.5 MeV photons. The neutrons were absorbed by CdCl_2 dissolved in water, which emitted photons within a few μs . The coincidence of these two kinds of photons confirmed the above reaction, and hence the presence of $\bar{\nu}_e$.

The discovery of ν_μ took place in 1962 at the Brookhaven National Laboratory [5] through the decays of pions. Iron from the USS battleship Missouri was used as the target. It was observed that the interactions of these neutrinos with the nuclei ($\nu_\mu/\bar{\nu}_\mu + N \rightarrow \mu^-/\mu^+ + N'$) produced only muons, but no electrons. This showed that the “muon” neutrinos produced in pion decay were distinct from the electron neutrinos produced in beta decays. This was an indication of “lepton flavour conservation” (which we now know does not hold true in general).

The direct observation of ν_τ took place only very recently, in 2000 at the DONUT experiment [6] at CERN. The main difficulty to be overcome here was identifying the τ produced in $\nu_\tau N \rightarrow \tau N'$ through its hadronic decays.

2.3 Measuring neutrino masses in experiments

The experiments with beta decay give an upper bound of 2.2 eV on the mass of “electron” neutrinos, as we have seen above.

The mass of “muon” neutrino can be determined by observing the energy of muon emitted in a pion decay at rest. It is a two-body decay, hence monoenergetic, and the energy is a direct function of the mass of the emitted neutrino. Unfortunately the accuracy in the energy measurement is not high enough to be able to determine the ν_μ mass: the current limit is of the order of 100 keV. The mass of ν_τ also has a measured upper bound of a few MeVs.

Two things are worth emphasizing here. Firstly, since we now know that the neutrino flavour eigenstates are very different from their mass eigenstates, it is not correct to use the phrase “mass of $\nu_e/\nu_\mu/\nu_\tau$ ”, and the above limits are to be taken in a very rough “pre-neutrino-mixing” spirit. Secondly, now that we know that the three mass eigenstates are very close (difference in mass squares is less than 10^{-2} eV^2), the mass limits of keV and MeV are no

longer relevant.

2.4 Parity violation

Another major development in the last century where neutrinos played an important role was the discovery of parity violation. In an attempt to solve the $\tau - \theta$ puzzle (both of which later turned out to be the same particle, K^+), Lee and Yang [7] proposed that parity is violated in the weak interactions. Experiments involving neutrinos soon verified this.

The experiment of Wu [8] consisted of putting ^{60}Co in a magnetic field and observing the forward - backward asymmetry of the electrons emitted from the beta decay. In the absence of parity violation, the asymmetry would have vanished. The observation of a nonzero asymmetry confirmed that parity is indeed violated.

The experiment of Telegdi [9] involved observing the angular distribution of electrons from the decay of polarized muons. This also confirmed parity violation.

Both the above experiments involved neutrinos, which violated parity maximally since only left handed neutrinos participate in weak interactions. This subsequently led to the $V - A$ model of weak interactions, which postulated the 4-Fermi interaction involving beta decay to be of the form

$$\frac{G_F}{\sqrt{2}}[\bar{p}\gamma_\mu(c_V - \gamma_5 c_A)n][\bar{e}\gamma^\mu(1 - \gamma_5)\nu] .$$

2.5 Interactions of neutrinos in SM

In SM, neutrinos interact only via weak interactions: they interact with W boson through the “charged current” interaction that gives rise to the term

$$\mathcal{L}_{CC} = [g/(2\sqrt{2})]\bar{\ell}\gamma^\mu(1 - \gamma_5)\nu W_\mu^- + h.c. \quad (3)$$

in the SM Lagrangian. The interaction with Z boson is the “neutral current” interaction that gives rise to the term

$$\mathcal{L}_{NC} = [g/(2 \cos \theta_W)]\bar{\nu}\gamma_\mu(1 - \gamma_5)\nu Z^\mu \quad (4)$$

in the SM Lagrangian. Note that the left-handed chiral projection operator $P_L \equiv (1 - \gamma_5)/2$ ensures that only left handed neutrinos $\nu_L \equiv [(1 - \gamma_5)/2]\nu$ and right handed antineutrinos $\bar{\nu}_R \equiv \bar{\nu}(1 + \gamma_5)/2$ take part in the interactions.

Since there is no right handed neutrino in the SM, neutrinos cannot get a mass through the interaction with a scalar, i.e. Higgs, like the other fermions.

2.6 Number of neutrino species

The Z boson decays into pairs of quarks and leptons. The decays to $q\bar{q}$ pairs and $\ell^+\ell^-$ pairs can be observed, whereas the decays to $\nu\bar{\nu}$ are “invisible”. By subtracting the “visible” decay width of Z (measured through the decay rates to visible channels) from the total Z width (determined from the Z lineshape), the decay rate of $Z \rightarrow \nu\bar{\nu}$ can be obtained. Knowing the decay rate to a single $\nu\bar{\nu}$ pair, one can determine the number of *active* neutrino species *with mass less than half the mass of Z* . The LEP experiment has given a very accurate measurement for the number of neutrino species: $N_\nu = 2.994 \pm 0.012$ [4].

2.7 Before neutrinos “became” massive

It should be clear from the above discussion that even before the current excitement in neutrino masses and mixing started, neutrinos played a crucial role in our understanding of the properties of matter. They were also a crucial ingredient of the deep inelastic scattering experiments that helped unravel the structure of protons and neutrons.

3 Atmospheric neutrinos: 2- ν mixing in vacuum

Although historically speaking, the first observations that made us suspect that neutrinos may have mass came from the solar neutrino experiments, the first confirmed evidence of neutrino masses came from the experiments that detected atmospheric neutrinos. In addition, the explanation of the atmospheric neutrino oscillations relies only on the neutrino propagation in vacuum and is not affected by matter. Therefore, we shall start with the observations of atmospheric neutrinos.

3.1 Atmospheric neutrino observations

The Earth is being constantly bombarded with cosmic rays that are mainly protons and come from all over the universe. The cosmic rays, upon interaction with the nuclei in the atmosphere, produce pions and kaons. Both pions and kaons decay predominantly into muons and muon neutrinos:

$$\pi^+ \rightarrow \mu^+ \nu_\mu, \quad \pi^- \rightarrow \mu^- \bar{\nu}_\mu, \quad K^+ \rightarrow \mu^+ \nu_\mu, \quad K^- \rightarrow \mu^- \bar{\nu}_\mu .$$

The muons then decay into electrons, one neutrino and one antineutrino:

$$\mu^- \rightarrow e^- \bar{\nu}_e \nu_\mu, \quad \mu^+ \rightarrow e^+ \nu_e \bar{\nu}_\mu .$$

As long as the detector does not distinguish between neutrinos and antineutrinos, this effectively means that the cosmic rays produce muon and electron neutrinos in the ratio 2:1.

The first hint that something is missing in our understanding of atmospheric neutrinos came from the observation that the muon-electron ratio was much smaller than 2. However, this was not enough to conclude that neutrinos were oscillating, since the “blame” could be shifted to the model dependence of the predictions of atmospheric neutrino fluxes.

The clinching evidence came in the form of the zenith angle dependence of neutrino fluxes. Fig. 1 shows the data from SuperKamiokande, which is a water Cherenkov detector. Here neutrinos are detected through their charged current interactions with electrons and nuclei in water.

The following features may be noted:

- Expected zenith angle distribution in the absence of oscillations: For sub-GeV events, the distribution in $\cos \Theta$ is flat, i.e. neutrino fluxes of both types are expected to be isotropic. For multi-GeV events, however, one expects a larger number of events coming from the $\cos \Theta \approx 0$ region, i.e. from near the horizon. The main factor influencing this is that the pions and muons produced by the cosmic rays get to travel more distance through the atmosphere and there is more chance of them decaying into neutrinos. The effect is virtually absent for sub-GeV events since the low energy pions / muons anyway have a small lifetime (in the frame of the Earth).
- The expected number of events is almost symmetric in $\cos \Theta$. The small deviation is due to the Earth’s magnetic field, and is well understood.

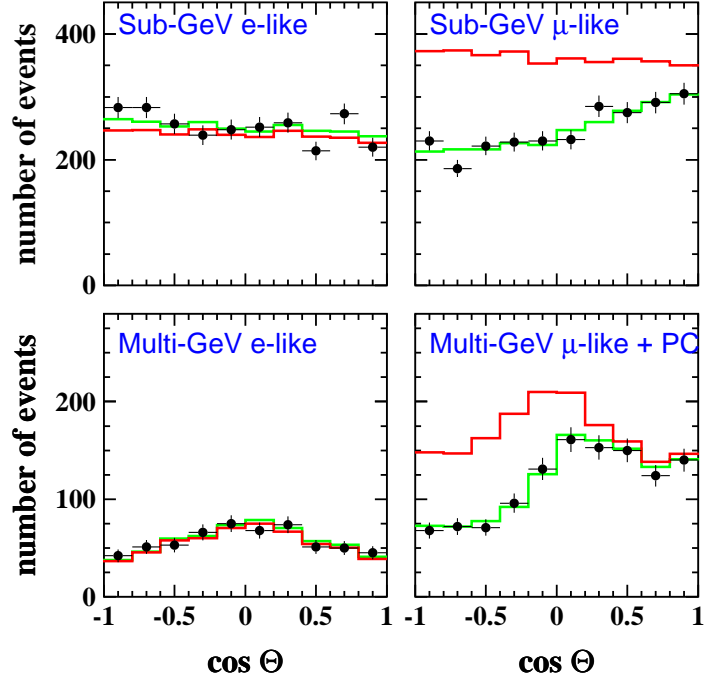


Figure 1: The zenith angle dependence of atmospheric neutrinos at SK

- The data for electron-like neutrino events matches with the expected number of events from Monte Carlo.
- The muon-like sub-GeV events are always less than expected, the depletion being greater for negative $\cos \Theta$, i.e. upcoming events.
- The muon-like multi-GeV events match with the expected rate for $\cos \Theta > 0$ (downgoing events), whereas a significant depletion is observed for the upcoming neutrinos.

Thus, the main observation is that the upcoming muon neutrinos suffer depletion. Since these neutrinos have to travel through much greater distances (~ 10000 km as opposed to ~ 10 km for downgoing neutrinos), this indicates that the depletion of neutrinos has a dependence on the distance travelled by them.

Since electron neutrinos do not seem to be affected, they must not be participating in the process. Therefore, if the muon neutrinos are getting converted to some other type of neutrinos, it has to be ν_τ . Let us see how the data can be explained through the ‘‘oscillations’’ of ν_μ into ν_τ .

3.2 Neutrino oscillations in vacuum

The effective Hamiltonian for a neutrino mass eigenstate with mass m_i is

$$H_i = \sqrt{p^2 + m_i^2} \approx p + \frac{m_i^2}{2p} \approx p + \frac{m_i^2}{2E} , \quad (5)$$

when only terms linear in (m_i/E) are kept. With neutrino masses less than eV and their energies in all relevant experiments of the order of MeV or above, this approximation is always valid. Since interference can take place only between neutrinos with the same p , we shall consider all neutrino fluxes as mixtures of coherent beams. For each coherent beam, the time evolution e^{-iHt} contains a common phase e^{-ipt} , which is irrelevant for oscillations. We shall therefore take the effective neutrino Hamiltonian to be

$$H_i = \frac{m_i^2}{2E} . \quad (6)$$

Let ν_α and ν_β be two neutrino flavour eigenstates. In general, they will not be mass eigenstates. Let the mass eigenstates be ν_1 and ν_2 with masses m_1 and m_2 respectively. The flavour eigenstates are a linear combination of mass eigenstates:

$$\begin{aligned} \nu_\alpha &= \cos \theta \nu_1 + \sin \theta \nu_2 \\ \nu_\beta &= -\sin \theta \nu_1 + \cos \theta \nu_2 . \end{aligned} \quad (7)$$

In general we denote it as

$$\nu_\alpha = \sum_i U_{\alpha i} \nu_i , \quad (8)$$

where ν_α is a flavour eigenstate, ν_i a mass eigenstate, and $U_{\alpha i}$ the mixing matrix. For two-neutrino mixing, U can be parametrized in terms of a single angle θ :

$$U = \begin{pmatrix} \cos \theta & \sin \theta \\ -\sin \theta & \cos \theta \end{pmatrix} . \quad (9)$$

If neutrinos are produced as a flavour eigenstate ν_α (like in the pion decay, for example), their time evolution will be

$$\begin{aligned} |\nu_\alpha(t)\rangle &= \cos\theta|\nu_1(t)\rangle + \sin\theta|\nu_2(t)\rangle \\ &= \cos\theta e^{-\frac{im_1^2 t}{2E}}|\nu_1(0)\rangle + \sin\theta e^{-\frac{im_2^2 t}{2E}}|\nu_2(0)\rangle \quad . \end{aligned} \quad (10)$$

The probability that we observe the same flavour eigenstate ν_α at time t is then

$$P_{\alpha\alpha} = |\langle\nu_\alpha|\nu_\alpha(t)\rangle|^2 = 1 - \sin^2 2\theta \sin^2\left(\frac{\Delta m^2 L}{4E}\right) \quad . \quad (11)$$

Here $\Delta m^2 \equiv m_2^2 - m_1^2$, and we have replaced t by L , the distance travelled, since neutrinos travel with the speed of light.

Eq. (11) is the standard formula for the “survival probability” of a neutrino flavour eigenstate when travelling through vacuum. Note that $P_{\alpha\alpha} = 1$ at $t = 0$ and it oscillates with a depth of $\sin^2 2\theta$ and an oscillation wavelength of $(4\pi E/\Delta m^2)$.

The “conversion probability” into the other flavour eigenstate ν_β is clearly

$$P_{\alpha\beta} = \sin^2 2\theta \sin^2\left(\frac{\Delta m^2 L}{4E}\right) \quad . \quad (12)$$

The above equation is in “natural” units, where $\hbar = c = 1$. If Δm^2 is in eV^2 , L in km and E in GeV, it may be written as

$$P_{\alpha\beta} = \sin^2 2\theta \sin^2\left(1.27 \frac{\Delta m^2(\text{eV}^2)L(\text{km})}{E(\text{GeV})}\right) \quad . \quad (13)$$

3.3 Explaining features of atmospheric neutrino data

The features of the atmospheric neutrino data pointed out earlier can now be explained using the oscillation hypothesis. Muon neutrinos are produced in the atmosphere and they “oscillate” into ν_τ during their propagation. This gives rise to the observed muon neutrino depletion.

- Electron neutrinos do not participate in the oscillations, hence their fluxes are not affected.

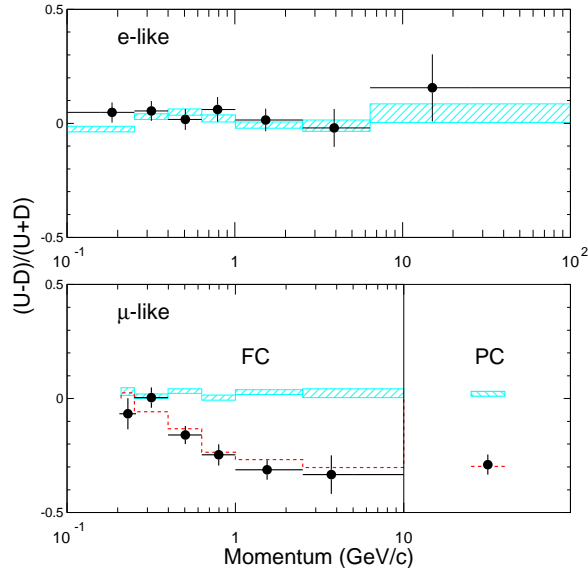


Figure 2: The up-down asymmetry in atmospheric neutrinos as a function of neutrino energy (momentum). Here U are the number of “upcoming” events with $\cos \Theta < -0.2$ and D are the number of “down-going” events with $\cos \Theta > 0.2$.

- Sub-GeV ν_μ oscillate with a small wavelength, so that even the height of the atmosphere is a significant fraction of the oscillation wavelength. The depletion is therefore observed at all values of the zenith angle, although more for upcoming neutrinos.
- Downgoing Multi-GeV neutrinos cannot oscillate in the small distance they travel in the atmosphere, and hence the depletion is very small. For the upgoing neutrinos, on the other hand, a larger distance is available and they undergo a significant depletion.

The above features also explain the up-down asymmetry shown in Fig. 2. The data may be fitted to eq. (11) for the two parameters Δm^2 and $\sin^2 2\theta$ [10].

$$\Delta m_{atm}^2 = (1.5 - 3.4) \times 10^{-3} \text{ eV}^2, \quad \sin^2 2\theta > 0.92 \quad (90\% \text{ C.L.})$$

Note that the oscillations take place with maximum depth ($\sin^2 2\theta \approx 1$). The situation $\theta = \pi/4$ is termed as maximal mixing. This is in contrast to the quark mixing, where the mixing angles are very small.

3.4 Ruling out other hypotheses

We have explained the depletion of atmospheric ν_μ by the hypothesis that they oscillate to ν_τ . However, the produced ν_τ have not yet been observed and therefore what we have shown above does not still rule out the possibility that ν_μ have oscillated to something else, for example a sterile neutrino species ν_s . This scenario can be ruled out by the data, but for that we need to examine the matter effects on neutrino mixing and oscillations.

Note that, even though the $\nu_\mu \leftrightarrow \nu_\tau$ oscillation hypothesis fits the data well, we have only observed the depletion of ν_μ . The appearance of ν_τ is yet to be seen. Moreover, in the absence of the observation of the “oscillations in L/E ”, i.e. a decrease and then an increase in the survival probability as a function of L/E , the hypothesis of neutrino decay would also give a reasonably good fit. Recently, SK announced such a “dip” in their L/E spectrum (see Fig. 3), which, if confirmed, will confirm the oscillation hypothesis without any doubt.

In order to confirm the atmospheric neutrino solution independently, one can produce ν_μ beams with known energies and fluxes and detect the ν_μ component left in them after travelling a certain distance. This experiment will not be affected by any model dependence in the calculation of atmospheric neutrino fluxes. The “short baseline” experiment K2K, where $\sim\text{GeV}$ ν_μ were produced and allowed to travel ~ 250 km to a detector, has confirmed the solution of the atmospheric neutrino anomaly. Two more experiments, MINOS (Fermilab to Minnesota) and CNGS (CERN to Gran Sasso) with baselines ~ 750 km, will start operating soon. The CNGS experiment also proposes to detect the ν_τ produced.

4 Two neutrino mixing in matter

In almost all physical situations, neutrinos have to travel through matter. This affects their effective masses and mixings, and has a profound impact on the flavour conversion probabilities.

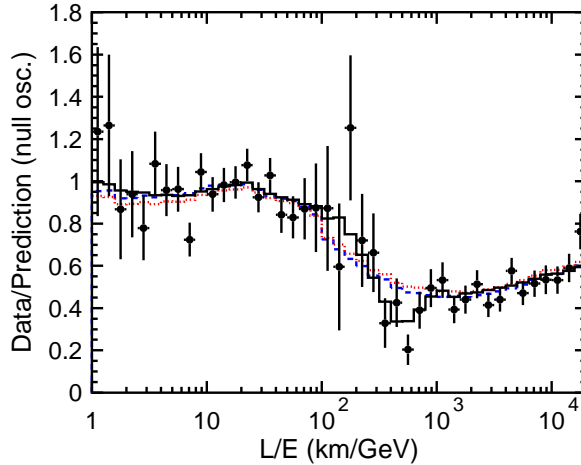


Figure 3: The “dip” in the L/E spectrum of atmospheric neutrinos, observed at SK.

4.1 Effective potentials in matter

When neutrinos travel through matter, the forward scattering interactions with electrons and nuclei give rise to effective potentials. All the neutrino flavour species undergo neutral current interactions, which give rise to an effective potential [11]

$$V_{NC} = -\frac{G_F}{\sqrt{2}}N_n \quad (14)$$

where N_n is the number density of neutrons in the medium. The neutral current potential V_{NC} is independent of the neutrino flavour.

Electron neutrinos undergo charged current interactions in addition to the neutral current ones, and hence have an additional effective charged current potential:

$$V_{CC} = \sqrt{2}G_F N_e \quad (15)$$

where N_e is the number density of electrons in the medium. Note that ν_μ and ν_τ do not have this effective potential.

4.2 Neutrinos in a constant matter density

Let us consider the mixing of ν_e with another neutrino flavour eigenstate, say ν_x . Here ν_x may be ν_μ , ν_τ or any linear combination of them. Since the effective potentials in matter are easier to write in the flavour basis, let us start by writing the effective Hamiltonian in the $(\nu_e \nu_x)$ flavour basis as

$$\begin{aligned} H_f &= U \begin{pmatrix} m_1^2/(2E) & 0 \\ 0 & m_2^2/(2E) \end{pmatrix} U^\dagger + \begin{pmatrix} V_{NC} & 0 \\ 0 & V_{NC} \end{pmatrix} + \begin{pmatrix} V_{CC} & 0 \\ 0 & 0 \end{pmatrix} \\ &= \begin{pmatrix} \frac{m_1^2}{2E} \cos^2 \theta + \frac{m_2^2}{2E} \sin^2 \theta & \frac{m_2^2 - m_1^2}{2E} \sin \theta \cos \theta \\ +V_{NC} + V_{CC} & \\ \frac{m_2^2 - m_1^2}{2E} \sin \theta \cos \theta & \frac{m_2^2}{2E} \cos^2 \theta + \frac{m_1^2}{2E} \sin^2 \theta + V_{NC} \end{pmatrix}. \end{aligned} \quad (16)$$

Since the mixing angle does not change when equal quantities are subtracted from all the diagonal elements, the above Hamiltonian is equivalent to

$$H_f = \frac{1}{4E} \begin{pmatrix} -\Delta m^2 \cos 2\theta + 2A & \Delta m^2 \sin 2\theta \\ \Delta m^2 \sin 2\theta & \Delta m^2 \cos 2\theta \end{pmatrix} \quad (17)$$

as far as the mixing angle and the difference between the eigenvalues is concerned. Here $\Delta m^2 \equiv m_2^2 - m_1^2$ and $A \equiv 2E V_{CC}$. The eigenvalues of the matrix (17) are

$$\begin{aligned} \frac{m_{1m}^2}{2E} &= \frac{1}{2E} \left(\frac{A}{2} - \frac{1}{2} \sqrt{(\Delta m^2 \cos 2\theta - A)^2 + (\Delta m^2 \sin 2\theta)^2} \right), \\ \frac{m_{2m}^2}{2E} &= \frac{1}{2E} \left(\frac{A}{2} + \frac{1}{2} \sqrt{(\Delta m^2 \cos 2\theta - A)^2 + (\Delta m^2 \sin 2\theta)^2} \right). \end{aligned} \quad (18)$$

Thus, the effective Δm^2 in matter becomes

$$\Delta m_m^2 \equiv m_{2m}^2 - m_{1m}^2 = \sqrt{(\Delta m^2 \cos 2\theta - A)^2 + (\Delta m^2 \sin 2\theta)^2}. \quad (19)$$

The effective Hamiltonian H_f can be diagonalized by a rotation matrix U as given in eq. (9), with the mixing angle θ_m in matter

$$\tan 2\theta_m = \frac{\Delta m^2 \sin 2\theta}{\Delta m^2 \cos 2\theta - A}. \quad (20)$$

An important thing to note here is that even if the mixing angle θ in vacuum were small, the matter effects can give rise to large (even maximal) effective mixing angle θ_m . This is called the MSW resonance [11, 12] (or “level crossing”), and occurs when

$$A = \Delta m^2 \cos 2\theta \quad . \quad (21)$$

In order to check whether matter effects play any significant role in neutrino propagation, it is enough to compare A with Δm^2 . For $A \ll \Delta m^2$, matter effects are virtually absent. When $A \gg \Delta m^2$, matter suppresses neutrino mixing ($\theta = \pi/2$).

In a medium of constant electron density, the effective values of Δm^2 and the mixing angle change, but the remaining dynamics stays the same as in the vacuum case. The flavour conversion probability, for instance, is

$$P_{\alpha\beta} = \sin^2 2\theta_m \sin^2 \left(\frac{\Delta m_m^2 L}{2E} \right) \quad . \quad (22)$$

4.3 Ruling out ν_s in atmospheric neutrino solution

Now we are in a position to distinguish between $\nu_\mu \leftrightarrow \nu_\tau$ and $\nu_\mu \leftrightarrow \nu_s$ oscillations in the atmospheric neutrinos. Since neutrinos coming with $\cos \Theta < 0$ have to pass through the Earth matter, there are potential matter effects. However for $\nu_\mu \leftrightarrow \nu_\tau$ oscillations, since both the species encounter the same effective potential V_{NC} , matter effects do not play any part. As a result, our earlier analysis in the absence of matter still stays valid.

On the other hand, in $\nu_\mu \leftrightarrow \nu_s$ oscillations, since the effective potential V_{NC} is absent for ν_s , net matter effects would be present. At high energies, where $\Delta m^2/(2E) < A$, these effects should be significant. The observation that no such matter effects are present even in the high energy neutrino events rules out $\nu_\mu \leftrightarrow \nu_s$ oscillations as the explanation of the atmospheric neutrino data.

4.4 Neutrinos through varying matter density

In many physical situations, neutrinos travel through varying matter densities. This has a very striking effect on their mixing, and the extent of flavour

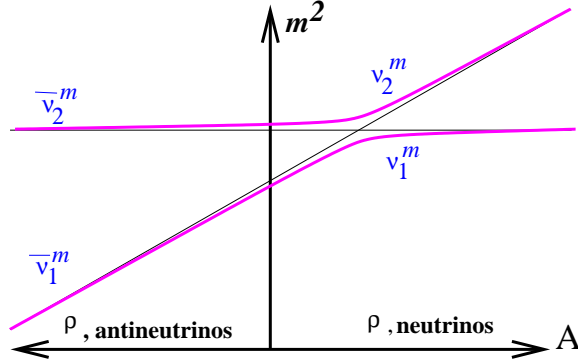


Figure 4: The values of Δm^2 as a function of A . The negative values of A correspond to antineutrinos. This is equivalent to Δm^2 as a function of ρ , with the negative half plane representing antineutrinos.

conversion depends not only on the matter density but how fast the density is changing.

The neutrinos produced by the nuclear reactions inside stars start their life in regions of very high densities and travel outwards to the surface of the stars and the interstellar space. As the matter density changes, so do the neutrino mass eigenstates ν_{im} . The propagation of neutrinos can be conveniently analyzed in the basis of these mass eigenstates. In many physical situations, the mass eigenstates may become decoherent, in which case their propagation may be studied independently.

The effective m^2 eigenvalues in matter (see eq. 18) as a function of A are shown in the “level crossing” diagram in Fig. 4. At extremely high densities, ν_e corresponds to ν_{2m} , the heavier mass eigenstate in matter.

Let $U(\theta_m)$ be the unitary matrix that diagonalizes the effective Hamiltonian *locally* in matter. Then we have

$$\begin{pmatrix} \nu_{1m} \\ \nu_{2m} \end{pmatrix} = U^\dagger(\theta_m) \begin{pmatrix} \nu_e \\ \nu_\mu \end{pmatrix} . \quad (23)$$

The Schrödinger’s equation then gives the evolution of the neutrino states as

$$i \frac{d}{dt} \begin{pmatrix} \nu_{1m} \\ \nu_{2m} \end{pmatrix} = i \frac{dU^\dagger(\theta_m)}{dt} \begin{pmatrix} \nu_e \\ \nu_\mu \end{pmatrix} + iU^\dagger(\theta_m) \frac{d}{dt} \begin{pmatrix} \nu_e \\ \nu_\mu \end{pmatrix}$$

$$\begin{aligned}
&= i \frac{dU^\dagger(\theta_m)}{dt} U(\theta_m) \begin{pmatrix} \nu_{1m} \\ \nu_{2m} \end{pmatrix} + U^\dagger(\theta_m) H_f U(\theta_m) \begin{pmatrix} \nu_{1m} \\ \nu_{2m} \end{pmatrix} \\
&= \begin{pmatrix} m_{1m}^2/(2E) & -id\theta_m/dt \\ id\theta_m/dt & m_{2m}^2/(2E) \end{pmatrix} \begin{pmatrix} \nu_{1m} \\ \nu_{2m} \end{pmatrix} . \tag{24}
\end{aligned}$$

In the limit of very slowly changing density, the off-diagonal elements in eq. (24) are much smaller than $|m_{2m}^2 - m_{1m}^2|/(2E)$, so that the mass eigenstates in matter, ν_{1m} and ν_{2m} , can be considered to be travelling independently, without mixing. This limit corresponds to

$$2d\theta_m/dt \ll |m_{2m}^2 - m_{1m}^2|/(2E) \tag{25}$$

which translates to

$$\frac{\Delta m^2}{(\Delta m_m^2)^2} \sin 2\theta \frac{dA}{dx} \ll \frac{\Delta m_m^2}{2E} \tag{26}$$

when we substitute for θ_m in matter. Clearly, the inequality is the weakest when Δm_m^2 is the smallest, which would happen at the resonance². The condition for ‘‘adiabaticity’’, i.e. for the mass eigenstates in matter not to mix, reduces to

$$\gamma \equiv \frac{\Delta m^2 \sin^2 2\theta}{2E \cos 2\theta} \left(\frac{1}{A} \frac{dA}{dx} \right)_{res}^{-1} \gg 1 \tag{27}$$

The probability of ‘‘jump’’ of one mass eigenstate in matter to another can be computed by using the WKB approximation [14]. The jump probability turns out to be approximately³.

$$P_{jump} = \text{Exp}(-\pi\gamma/2) \tag{28}$$

The jump probability thus depends on Δm^2 , mixing angle, the density profile encountered by the neutrinos, as well as the neutrino energy.

Note that the WKB approximation allows us to calculate only the probability of neutrino conversion, so it is valid only as long as the mass eigenstates are decoherent. This condition is satisfied in particular by the solution of the solar neutrino anomaly [15].

²A more accurate analysis has been done in [13].

³Strictly speaking, this expression is valid only for linear density profiles and small mixing angles, but it can describe almost all the situations of interest well. The corrections can be computed as shown in [14].

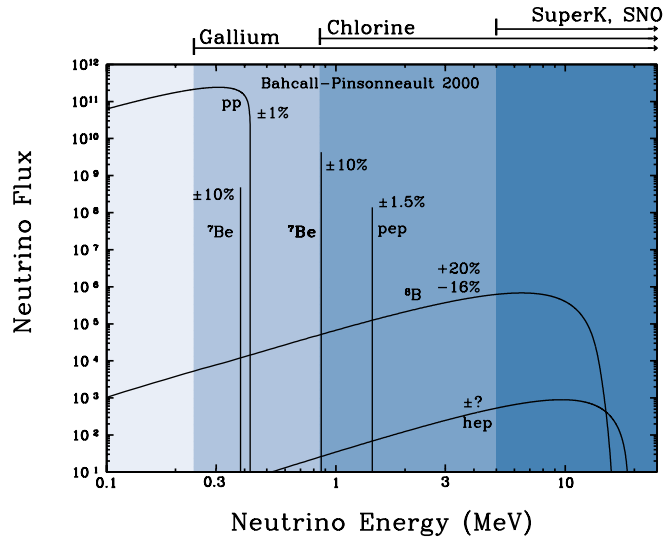


Figure 5: The solar neutrino fluxes predicted in the SSM

5 Solar neutrinos: problem and solution

5.1 Standard solar model and missing neutrinos

The sun shines because of the nuclear fusion reactions that take place inside its core. The major reaction is $4p \rightarrow {}^4\text{He} + 2e^+ + 2\nu_e$, though there are other reactions that produce heavier elements like Be , B and give off ν_e . This is the only neutrino species that can be produced in these nuclear reactions. The energies of these ν_e are $\sim (0.1 - 15)$ MeV.

Fig. 5 shows the energy spectra of neutrinos produced in various reactions inside the sun, according to the standard solar model (SSM). The electroweak theory predicts the shapes of the spectra, but the absolute magnitudes of the fluxes are calculated from the SSM [16, 17].

The first indication that something was missing came from the observation of solar neutrinos through radiochemical reactions. Gallium and chlorine were the two nuclei used, which would absorb ν_e and convert to radioactive nuclei with the lifetime of the order of a few weeks. Periodically the num-

ber of radioactive nuclei from the detector would be counted, which would then give the total flux of ν_e from the sun. The two detection reactions have two different thresholds, and hence probe different regions of the neutrino spectra, as shown in the figure.

The relevant radiochemical reactions and their threshold energies are:

$$\text{Gallium : } {}^{71}\text{Ga} + \nu_e \rightarrow {}^{71}\text{Ge} + e^- \quad (233 \text{ keV}) \quad , \quad (29)$$

$$\text{Chlorine : } {}^{37}\text{Cl} + \nu_e \rightarrow {}^{37}\text{Ar} + e^- \quad (814 \text{ keV}) \quad . \quad (30)$$

In addition, in water Cherenkov detectors like Kamiokande (and later Super-Kamiokande), ν_e were detected through the “elastic scattering” processes

$$\nu_e + e^- \rightarrow \nu_e + e^- \quad , \quad (31)$$

where the electron was detected through its Cherenkov radiation. The threshold for the detection through this process is around 5 MeV, the limiting factor here being the rejection of the background noise in the photomultiplier tubes.

The combined observations of these experiments suggested that the flux of ν_e from the sun was smaller than expected by almost a factor of two. Changing the relative flux ratios between ν_e from different reactions also did not help matters. A detailed description of the solar neutrino problem can be found in [18]. Here I shall just point out some salient features of the solution of the problem through neutrino mixing.

5.2 Zooming in on the solar neutrino solution

Neutrinos are produced inside the core of the sun, where $A \gg \Delta m^2/(2E)$, so that $\theta_m \approx \pi/2$ and $\nu_e \approx \nu_{2m}$. The neutrinos, on their way out to the surface of the sun, encounter a level crossing where some of the ν_{2m} would jump to ν_{1m} . Depending on the jump probability P_L , the probability that a ν_e is observed at the detector is

$$P_{ee} = P_L \cos^2 \theta + (1 - P_L) \sin^2 \theta \quad , \quad (32)$$

where θ is the mixing angle in vacuum. P_L is a function of $\Delta m^2, \theta$ and the density profile, as shown in eq.(28).

Using the detected ν_e fluxes and their energy dependence, the allowed regions in the $(\Delta m^2 - \tan^2 \theta)$ parameter space (using the data till 2001) are

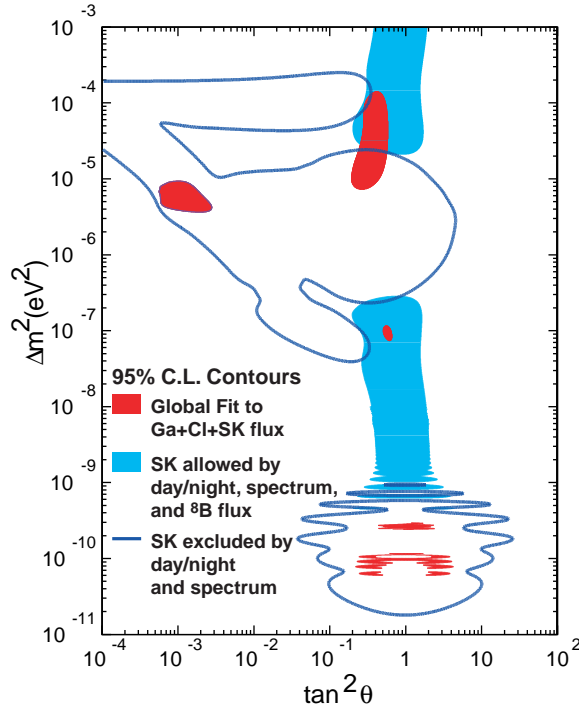


Figure 6: Allowed regions in the parameter space for solar neutrino solution with data till 2001

shown in Fig. 6. Though the fit shown in the figure is outdated now, it is instructive to notice some salient features of the solutions that the data allowed at that time.

The two solutions with $\Delta m^2 > 10^{-6} \text{ eV}^2$ are the MSW solutions, where the neutrino flavour conversions are dominated by the dynamics in the resonance layer inside the sun. The solutions correspond to the SMA (small mixing angle) where $\theta \ll 1$ but $P_L \sim 1$ and LMA (large mixing angle) where $\theta \sim 1$ but $P_L \approx 0$. For both these solutions, Δm^2 is large enough to cause a complete decoherence between the mass eigenstates ν_{1m} and ν_{2m} . The solution with $\Delta m^2 \sim 10^{-7} \text{ eV}^2$, the so-called LOW solution, is another MSW solution with $\theta \sim 1$ and $P_L \sim 1$.

The solution near $\Delta m^2 \sim 10^{-10} \text{ eV}^2$ is the VAC (vacuum oscillation)

solution, where the resonance inside the sun is completely nonadiabatic ($P_L \approx 1$) and the oscillations take place between the sun and the earth, with the oscillation wavelength comparable to the sun-earth distance. The coherence between the mass eigenstates is maintained in this case.

Data in the past few years have ruled out the SMA, LOW and VAC solution, whereas the LMA solution has been confirmed. Some of the observations instrumental in ruling out the other solutions were:

- VAC solution implies that the oscillation probability, measured through eq.(11) depends on the distance of the earth from the sun, and therefore would change seasonally as the earth moves around the sun in an elliptic orbit. This seasonal variation has not been observed.
- SMA solution implies significant day-night effects: at night, the neutrinos from the sun pass through the earth matter before reaching the detector, which leads to a significant change in the ν_e survival probability. The observed difference in the neutrino fluxes during day and night is much smaller than what this solution predicts.
- Both the VAC and the SMA solution imply an energy dependence of the ν_e survival probability: the VAC solution through the $\sin^2(\Delta m^2 L/E)$ term and the SMA solution through the energy dependence of P_L , [in turn through the energy dependence of γ in eq. (27)]. The LMA solution gives $P_L = 0$ throughout the energy range $E > 5$ MeV and hence predicts no energy dependence. The data, as shown in Fig. 7, show no energy dependence for $E > 5$ MeV, thus strongly favouring the LMA solution and ruling out the other two. Note that even the LMA solution has an energy dependence at low energies, so that the Ga and Cl “radiochemical” experiments give a smaller survival probability.

Note that the observations above have been given just to gain some physical insight into what is happening. The actual parameter values are determined by a fit to all the data, using parameters that include $\Delta m^2, \theta$ and the ratios of fluxes from various reactions. The LOW solution is also eliminated through the combined fit.

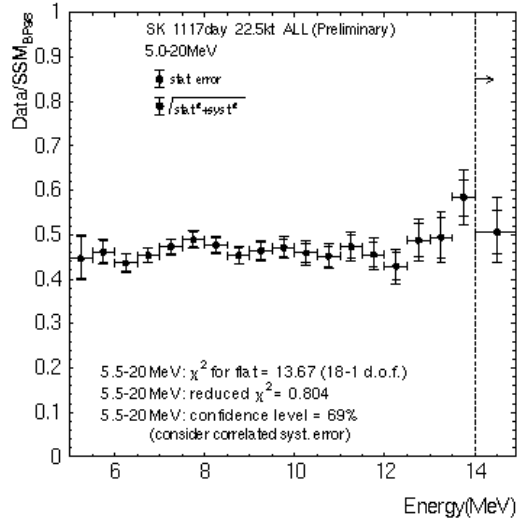


Figure 7: Observed survival probability of solar ν_e as a function of energy.

5.3 Where do the solar ν_e go ?

The oscillation hypothesis that explains the solar neutrino observations involves the conversion of ν_e into ν_μ, ν_τ or some linear combination of them. However, the experiments mentioned above are not able to confirm that the ν_μ or ν_τ are indeed produced. That evidence came from the SNO (Sudbury Neutrino Observatory) experiment that used heavy water as the detector, and detected neutrinos through three reactions:

- Elastic scattering (ES) $\nu + e^- \rightarrow \nu + e^-$: This reaction detects all three neutrino species, ν_e, ν_μ and ν_τ . However, the cross section of the reaction involving ν_e is almost 6 times the cross section of the reaction involving the other two species, so that this reaction can be said to be sensitive to the combination of fluxes $\Phi_e + \Phi_{\mu+\tau}/6$.
- Charged current (CC) $\nu_e + d \rightarrow p + p + e^-$: This reaction can take place only with ν_e , and hence is sensitive to Φ_e .
- Neutral current (NC) $\nu + d \rightarrow n + p + \nu$: This reaction is blind to the flavour of the neutrino species and hence effectively measures $\Phi_e + \Phi_{\mu+\tau}$.

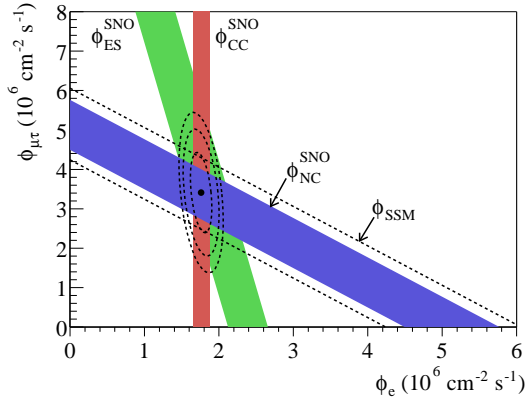


Figure 8: The results from SNO on various linear combinations of ν_e and $\nu_{\mu/\tau}$ fluxes.

In SNO, the NC process was detected through the addition of salt to the heavy water, which was useful in capturing neutrons. The observations, shown in Fig. 8, confirmed that *all* the disappearing ν_e were indeed getting converted to ν_μ or ν_τ . This ruled out the conversion of ν_e to a sterile fermion as the mechanism for the solar neutrino oscillations.

The neutral current data also matched with the fluxes predicted by SSM, thus vindicating SSM as the correct model of the solar dynamics.

5.4 Confirming the solar neutrino solution on earth

With the solar parameters approximately known, it was possible to confirm them using a neutrino source on the earth and observing the depletion of the flux after the neutrinos travel a known distance. The $\bar{\nu}_e$ that are produced in nuclear reactors have energies of a few MeV, and hence with the oscillation parameters obtained by the solar neutrino fit, an oscillation length in vacuum of ~ 100 km. The oscillation parameters can then be tested by having a detector at the appropriate distance from the source.

The KamLand experiment, which used the combined flux of many nuclear reactors in Japan and a scintillation detector, confirmed the LMA solution and measured the values of Δm^2 and θ to a much better accuracy. The best

fit values for the mixing parameters are [19]

$$\Delta m_{\odot}^2 = (7.2 - 9.5) \times 10^{-5} \text{eV}^2 \quad , \quad \sin^2 \theta_{\odot} = 0.21 - 0.37 \quad (3\sigma) \quad (33)$$

The LMA solution, confirmed by all the experimental data, corresponds to (for $E > 5$ MeV) a completely adiabatic transition ($P_L = 0$) at the resonance the neutrinos undergo inside the sun. Thus, ν_e , which are produced as ν_{2m} inside the sun, travel through the matter inside the sun and emerge from the sun as ν_2 . These ν_2 , being mass eigenstates in vacuum, reach the earth as ν_2 , where they are detected as ν_e with a probability $\sin^2 \theta$ and as $\nu_{\mu/\tau}$ with a probability $\cos^2 \theta$.

6 Three neutrino mixing

Since ν_e do not participate in the atmospheric neutrino oscillations, whereas they do participate in the solar neutrino oscillations, it is clear that in order to have a consistent picture of neutrino mixings, we have to develop a framework for the mixing of all three neutrino species, $\nu_e, \nu_{\mu}, \nu_{\tau}$. We express these flavour eigenstates as linear combinations of the three mass eigenstates in vacuum, ν_1, ν_2, ν_3 as

$$\nu_{\alpha} = \sum_i U_{\alpha i} \nu_i \quad , \quad (34)$$

where the mixing matrix U can be parametrized as a product of three rotation matrices:

$$U = R_{23}(\theta_{23})R_{13}(\theta_{13})R_{12}(\theta_{12}) \quad . \quad (35)$$

We neglect CP violation for the moment, and shall introduce it in the later section. In the absence of CP violation, the 3×3 mixing matrix is real and is completely described in terms of the three mixing angles, $\theta_{12}, \theta_{13}, \theta_{23}$. It can be explicitly written as

$$\begin{aligned} U &= \begin{pmatrix} 1 & 0 & 0 \\ 0 & c_{23} & s_{23} \\ 0 & -s_{23} & c_{23} \end{pmatrix} \begin{pmatrix} c_{13} & 0 & s_{13} \\ 0 & 1 & 0 \\ -s_{13} & 0 & c_{13} \end{pmatrix} \begin{pmatrix} c_{12} & s_{12} & 0 \\ -s_{12} & c_{12} & 0 \\ 0 & 0 & 1 \end{pmatrix} \\ &= \begin{pmatrix} c_{12}c_{13} & s_{12}c_{13} & s_{13} \\ -s_{12}c_{23} - c_{12}s_{23}s_{13} & c_{12}c_{23} - s_{12}s_{23}s_{13} & s_{23}c_{13} \\ s_{12}s_{23} - c_{12}c_{23}s_{13} & -c_{12}s_{23} - s_{12}c_{23}s_{13} & c_{23}c_{13} \end{pmatrix} \quad , \quad (36) \end{aligned}$$

where $c_i \equiv \cos \theta_i$ and $s_i \equiv \sin \theta_i$.

The probability that a neutrino flavour eigenstate ν_α will be converted to another flavour eigenstate ν_β can be calculated as we had seen in the case of two neutrino mixing.

$$\begin{aligned}
P_{\alpha\beta} &= \delta_{\alpha\beta} - 4 \sum_{i>j} \text{Re}(U_{\alpha i}^* U_{\beta i} U_{\alpha j} U_{\beta j}^*) \sin^2 \left(\frac{\Delta m_{ij}^2 L}{4E} \right) \\
&\quad + 2 \text{Im}(U_{\alpha i}^* U_{\beta i} U_{\alpha j} U_{\beta j}^*) \cos \left(\frac{\Delta m_{ij}^2 L}{2E} \right) .
\end{aligned} \tag{37}$$

With no CP violation, the last term vanishes.

6.1 Measurement of θ_{13}

Only an upper limit on θ_{13} is currently available, the best limit is from the experiment CHOOZ [20] that determines the survival probability of $\bar{\nu}_e$ after propagation in vacuum for a fixed distance L . The survival probability is

$$\begin{aligned}
P_{ee} &= 1 - 4U_{e1}^2 U_{e2}^2 \sin^2(\Delta m_{21}^2 L/4E) - \\
&\quad 4U_{e2}^2 U_{e3}^2 \sin^2(\Delta m_{32}^2 L/4E) - 4U_{e1}^2 U_{e3}^2 \sin^2(\Delta m_{31}^2 L/4E) \\
&\approx 1 - 4U_{e3}^2 (1 - U_{e3}^2) \sin^2(\Delta m_{32}^2 L/4E) ,
\end{aligned} \tag{38}$$

where we have neglected the term containing $\sin^2(\Delta m_{21}^2 L/4E)$ because of its smallness (L/E was chosen such that the term is small in magnitude), used $\Delta m_{32}^2 \approx \Delta m_{31}^2$, and used the unitarity of the mixing matrix, which implies

$$U_{e1}^2 + U_{e2}^2 + U_{e3}^2 = 1 . \tag{39}$$

The observations could give only a lower bound on P_{ee} , which corresponds to an upper bound on $4U_{e3}^2(1 - U_{e3}^2) = \sin^2 2\theta_{13}$. This bound corresponds to two possible solutions, one with $\theta_{13} \approx 0$ and the other with $\theta_{13} \approx \pi/2$. The later solution, which corresponds to $|U_{e3}| \approx 1$, is ruled out since that would not allow $|U_{\mu 3}|$ to be large enough to give rise to the observed atmospheric neutrino oscillations.

The actual limit by the CHOOZ experiment depends on the value of Δm_{31}^2 , the dependence being strong at low Δm_{31}^2 values as shown in Fig. 9. With the current values of atmospheric neutrino parameters, the upper bound is $\sin^2 \theta_{13} < 0.05$ (3σ).

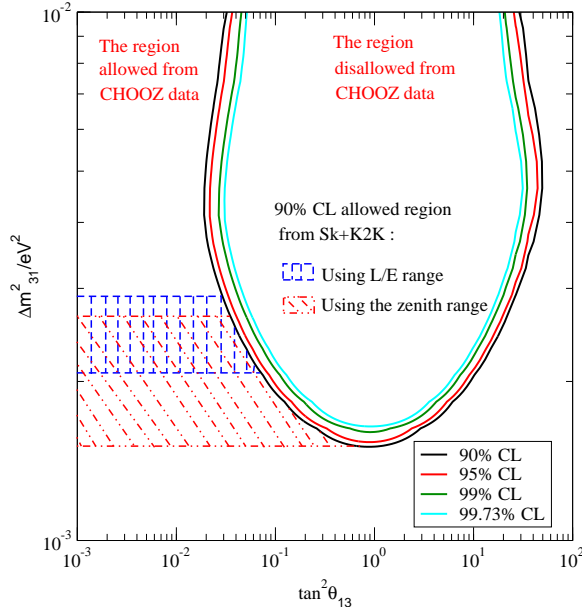


Figure 9: The allowed range for θ_{13} from CHOOZ data [19].

6.2 Solar and atmospheric neutrinos in 3ν framework

We already know that $\Delta m_{\odot}^2 \ll \Delta m_{atm}^2$. The neutrino mass spectrum thus consists of two mass eigenstates relatively close together (separated by Δm_{\odot}^2) and one mass eigenstate comparatively further away from these two. We define the eigenstate further away by ν_3 . Out of the remaining two eigenstates, the heavier one is ν_2 and the lighter one ν_1 , by definition.

The atmospheric neutrinos measure the survival probability of ν_{μ} in vacuum, i.e.

$$\begin{aligned}
 P_{\mu\mu} &= 1 - 4U_{\mu 1}^2 U_{\mu 2}^2 \sin^2(\Delta m_{21}^2 L/4E) - \\
 &\quad 4U_{\mu 2}^2 U_{\mu 3}^2 \sin^2(\Delta m_{32}^2 L/4E) - 4U_{\mu 1}^2 U_{\mu 3}^2 \sin^2(\Delta m_{31}^2 L/4E) \\
 &\approx 1 - 4U_{\mu 3}^2 (1 - U_{\mu 3}^2) \sin^2(\Delta m_{32}^2 L/4E) \quad , \quad (40)
 \end{aligned}$$

where we have neglected the term containing $\sin^2(\Delta m_{21}^2 L/4E)$ because of its

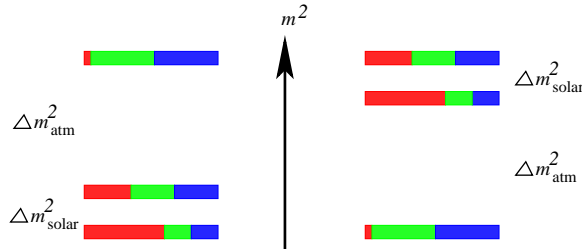


Figure 10: The normal (left) and inverted (right) hierarchy. The red, green and blue colours (dark grey, light grey, black for greyscale) stand for the ν_e, ν_μ and ν_τ components in the respective mass eigenstates.

smallness, used $\Delta m_{32}^2 \approx \Delta m_{31}^2$, and used the unitarity of the mixing matrix:

$$U_{\mu 1}^2 + U_{\mu 2}^2 + U_{\mu 3}^2 = 1 \quad . \quad (41)$$

Since $\cos \theta_{13} \approx 1$, we have $4U_{\mu 3}^2(1 - U_{\mu 3}^2) \approx \sin^2 2\theta_{23}$. Comparing the survival probability with the one obtained in eq.(11) using two neutrino mixing, we get

$$\theta_{atm} \approx \theta_{23} \quad (42)$$

so that the atmospheric neutrino observations give

$$\Delta m_{atm}^2 \approx |\Delta m_{31}^2| \approx 2 \times 10^{-3} \text{eV}^2, \quad \theta_{atm} \approx \theta_{23} \approx 45^\circ \quad . \quad (43)$$

Note that only the magnitude of Δm_{31}^2 is measured in the atmospheric neutrino experiments, and not its sign. As a result, there are two possible mass hierarchies in neutrinos, one “normal” where $m_1 < m_2 < m_3$ and the other “inverted” where $m_3 < m_1 < m_2$. The hierarchies are shown in Fig. 10.

In the case of solar neutrino solution, using $\theta_{13} \approx 0$ one can show that

$$\Delta m_{\odot}^2 \approx \Delta m_{21}^2 \approx 8 \times 10^{-5} \text{eV}^2, \quad \theta_{\odot} \approx \theta_{12} \approx 32^\circ \quad . \quad (44)$$

Thus, due to the smallness of θ_{13} and the “hierarchy” in Δm^2 , the solutions to the solar and atmospheric neutrino anomalies are completely decoupled, and have a simple correspondence with the angles that parametrize the mixing matrix.

The measurement of θ_{13} and determining the sign of Δm_{31}^2 are two of the important future challenges for neutrino experiments.

6.3 More than three neutrino species ??

The LSND experiment [21] has announced the observation of $\bar{\nu}_\mu \rightarrow \bar{\nu}_e$ oscillations that correspond to $\Delta m^2 \approx (0.1 - 10) \text{ eV}^2$. Such a large value of Δm^2 cannot be fitted into the current framework of three neutrino oscillations. The LSND observations have not yet been confirmed by other experiments, but if confirmed, it would imply that we need another mass eigenstate, and hence another flavour eigenstate. Since we know that there are only three light active flavour eigenstates (see Sec. 2.6), the fourth flavour eigenstate ν_s must be a “sterile” one, i.e. not having any standard model interactions.

Given that now we have three independent Δm^2 that are hierarchical ($\Delta m_\odot^2 \ll \Delta m_{atm}^2 \ll \Delta m_{LSND}^2$), the neutrino mass spectrum could be of two forms: the so-called 2+2 and 3+1 schemes.

In the “2+2” scheme, ν_2 and ν_3 are separated by Δm_{atm}^2 , ν_1 and ν_4 by Δm_\odot^2 , and these two pairs are separated by Δm_{LSND}^2 . In this scheme, the atmospheric neutrino solution remains unaffected, whereas the solar neutrino solution has to be through the mixing of ν_e with ν_s . The observations from SNO, which detect the production of $\nu_{\mu/\tau}$ from solar neutrinos, disfavour this solution.

Another (disfavoured) version of the “2+2” scheme is when ν_3 and ν_4 are separated by Δm_{atm}^2 , ν_1 and ν_2 by Δm_\odot^2 , and these two pairs are separated by Δm_{LSND}^2 . This implies that the atmospheric neutrino anomaly should be explained through $\nu_\mu - \nu_s$ oscillations, which is disfavoured as explained in Sec. 4.3.

In the “3+1” scheme, the states ν_1, ν_2, ν_3 are as in the standard three neutrino mixing picture, and ν_4 is separated from them by Δm_{LSND}^2 . In this picture, the LSND observations give a lower bound on the combination $U_{e4}^2 U_{\mu 4}^2$, which conflicts with the lower bound on the same combination given by the CHOOZ experiments.

The scenarios with an additional sterile neutrino thus fail to describe all the experiments simultaneously. There are still some ways to get around this by adding more sterile neutrinos, but let us not get into that.

7 Dirac vs. Majorana neutrinos

When Lorentz boosted with a large velocity opposite to its motion, a left handed massive particle becomes a right handed one. Since neutrinos have mass, ν_L would go into ν_R , a right handed particle. A priori, there is nothing preventing this ν_R from being the same as $\bar{\nu}_R$, which is already known to exist. In other words, it is possible for the neutrino to be its own antiparticle. One might argue that the lepton number conservation would not allow such a possibility, however lepton number conservation is just an accidental symmetry of the standard model and not crucial to its gauge structure.

If neutrino is its own antiparticle, it is termed as a Majorana neutrino. It clearly has only two independent spinor components as contrasted with the other standard model fermions, which are 4-component Dirac spinors. In particular, the positive and negative energy solutions of the Dirac equation for the neutrinos are related. (See [1, 2].)

The charge conjugate state of a fermion f can be defined in a way that makes sure that it transforms like f under Lorentz transformations:

$$f^c \equiv -\eta_c^* C \bar{f}^T = -\eta_c^* i \gamma^2 f^* \quad , \quad (45)$$

where η_c is a “creation” phase, and $C \equiv i \gamma^2 \gamma^0$ can be written in terms of the Dirac matrices [1].

A Majorana neutrino that is the same as its antiparticle can be constructed as

$$\nu_M \equiv \nu_L + \nu_L^c \quad , \quad (46)$$

where ν_L^c is to be understood as $(\nu_L)^c$. The presence of such a neutrino, which does not have a well-defined lepton number (since the lepton numbers for ν_L and ν_L^c are opposite), ensures that lepton number is not a conserved quantity. Such a neutrino can have a “Majorana mass” term in the lagrangian,

$$\mathcal{L}_M \equiv -m_M \bar{\nu}_M \nu_M = -m_M (\bar{\nu}_L^c \nu_L + \bar{\nu}_L \nu_L^c) \quad , \quad (47)$$

which breaks the lepton number symmetry explicitly.

If the lepton number is conserved, the only mass term for the neutrinos allowed in the Lagrangian would be

$$\mathcal{L}_D \equiv -m_D (\bar{\nu}_L \nu_R + \bar{\nu}_R \nu_L) \quad , \quad (48)$$

the ‘‘Dirac mass’’ term. Note that this requires the existence of a right handed neutrino ν_R in addition to the standard model ν_L , as opposed to the Majorana case where no extra particle is needed.

7.1 Neutrinoless double beta decay

The experiments involving neutrino oscillations cannot identify whether neutrino is a Majorana particle. However, a potential reaction which, if observed, would confirm the Majorana nature of neutrino is the neutrinoless double beta decay:

$$N(A, Z) \rightarrow N'(A, Z + 2) + 2e^- \quad (49)$$

where the nucleus N with atomic mass number A and atomic number Z decays to the nucleus N' with atomic mass number A and atomic mass number $Z + 2$ without any neutrino emission (i.e. without any missing energy). Such a reaction is characterized by the two electrons emitted back to back with the same energy, the combined energy being exactly equal to the Q value of the reaction.

The cross section for this process is proportional to a particular combination of Majorana masses:

$$\sigma \propto \left| \sum U_{ei}^2 m_i \right|^2, \quad (50)$$

so that the number of events observed are a measure of the ‘‘effective’’ Majorana mass of the electron neutrino:

$$\langle m_{ee} \rangle \equiv \left| \sum U_{ei}^2 m_i \right|. \quad (51)$$

Till now no confirmed neutrinoless double beta decay events have been observed, which has enabled us to put an upper bound of $\langle m_{ee} \rangle < 0.35$ eV (90% C.L.) [22].

7.2 Combining Dirac and Majorana masses

In general, both the Dirac and Majorana mass terms may be present in the Lagrangian of a theory. Of course, this implies that the theory has right handed neutrinos, and also incorporates lepton number violation. We shall see one example, which can give us some insight into the mechanism of neutrino mass generation.

The Lagrangian is

$$\mathcal{L} = -m_D \overline{\nu}_L \nu_R - \frac{1}{2} (m_L \overline{\nu}_L^c \nu_L + m_R \overline{\nu}_R^c \nu_R) + h.c. \quad . \quad (52)$$

Denoting $\nu \equiv \left(\nu_L \quad \nu_R^c \right)^T$, the Lagrangian may be written as

$$\mathcal{L} = -\frac{1}{2} \overline{\nu}^c \mathcal{M} \nu + h.c. \quad , \quad (53)$$

where

$$\mathcal{M} = \begin{pmatrix} m_L & m_D \\ m_D & m_R \end{pmatrix} \quad . \quad (54)$$

This matrix has eigenvalues of

$$\begin{aligned} m_1 &= \frac{1}{2} \sqrt{4m_D^2 + (m_R - m_L)^2} - \frac{m_R + m_L}{2} \quad , \\ m_2 &= \frac{1}{2} \sqrt{4m_D^2 + (m_R - m_L)^2} + \frac{m_R + m_L}{2} \quad . \end{aligned} \quad (55)$$

A few extreme cases are interesting.

- When $m_D \gg m_L, m_R$, we have two quasi-degenerate neutrino mass eigenstates, with a mixing angle of 45° , i.e. ν_L and ν_R^c mix maximally. Such a scenario is called “pseudo-Dirac neutrinos”.
- When $m_R \gg m_D, m_L$, it is the so-called “seesaw” scenario. The special case when $m_L = 0$ is the “Type I” seesaw. This implies

$$m_1 \approx m_D^2/m_R \quad , \quad m_2 \approx m_R \quad , \quad (56)$$

so that heavier m_R corresponds to lighter m_1 and vice versa (hence the term “seesaw”). In scenarios with quark-lepton unification, where m_D for neutrinos is expected to be of the same order as the Dirac mass matrix for the up-type quarks, sub-eV neutrino masses can be obtained by having $m_R \sim 10^9$ GeV. The seesaw mechanism has been employed in many neutrino mass models.

When $m_L \ll m_R$ but nonvanishing, it is “Type II” seesaw. In this case, the mass of the light neutrino is determined by m_L , but the mixing with the heavier neutrino is governed by m_D/m_R .

For a detailed discussion of some of these scenarios, the reader is referred to [2].

7.3 CP violation in neutrinos

The CP violation in the lepton sector can be described in the same way as that in the quark sector: the charged current interaction term in the Lagrangian is

$$\mathcal{L}_{CC} = (g/\sqrt{2})(\bar{\ell}_L \gamma^\mu \nu_L W_\mu^- + h.c.) \quad (57)$$

where ℓ_L and ν_L are three-vectors of charged lepton and neutrino flavour eigenstates respectively. Writing this in terms of mass eigenstates of the charged leptons and neutrinos gives

$$\mathcal{L}_{CC} = (g/\sqrt{2})(\bar{E}_L U_\ell^\dagger \gamma^\mu U_\nu N_L W_\mu^- + h.c.) \quad (58)$$

$$= (g/\sqrt{2})(\bar{E}_L \gamma^\mu V_{PMNS} N_L W_\mu^- + h.c.) \quad , \quad (59)$$

where $V_{PMNS} \equiv U_\ell^\dagger U_\nu$ is the lepton mixing matrix, named after Pontecorvo, Maki, Nakagawa and Sakata. The matrices U_ℓ and U_ν are the ones that diagonalize the charged lepton and neutrino mass matrices respectively in their flavour basis.

The matrix V_{PMNS} is a 3×3 unitary matrix, implying that it has 9 independent parameters. If neutrinos are Dirac particles, the relative phases of both the left handed charged leptons and left handed neutrinos can be chosen arbitrarily (since they can be absorbed by the corresponding right handed particles that do not participate in the charged current interactions), and eliminating these 5 relative unphysical phases leaves V with 4 independent parameters. Only three of these can be real, since any 3×3 real unitary matrix can be written in terms of a maximum of 3 parameters. The matrix V thus has to be complex. This complex nature of V gives rise to CP violation.

If we use the basis where the charged lepton mass matrix is diagonal, V_{PMNS} is the same as the neutrino mixing matrix U_ν . Including the complex phase parameter δ that gives rise to CP violation, the mixing matrix V (or U_ν) can be written as

$$V = R_{23}(\theta_{23})\Phi(\delta)R_{13}(\theta_{13})\Phi^\dagger(\delta)R_{12}(\theta_{12}) \quad (60)$$

where $\Phi(\delta) \equiv \text{Diag}[1, 1, e^{i\delta}]$. Note that this is just a convention that reproduces the standard form of the quark mixing matrix in PDG:

$$V = \begin{pmatrix} c_{12}c_{13} & s_{12}c_{13} & s_{13}e^{-i\delta} \\ -s_{12}c_{23} - c_{12}s_{23}s_{13}e^{i\delta} & c_{12}c_{23} - s_{12}s_{23}s_{13}e^{i\delta} & s_{23}c_{13} \\ s_{12}s_{23} - c_{12}c_{23}s_{13}e^{i\delta} & -c_{12}s_{23} - s_{12}c_{23}s_{13}e^{i\delta} & c_{23}c_{13} \end{pmatrix} . \quad (61)$$

If neutrinos were Majorana particles, the term \mathcal{L}_M in the Lagrangian [see eq. (47)] disallow the freedom of changes of phases of neutrinos. As a result, only the three unphysical phases of the charged leptons can be eliminated from V , leaving the mixing matrix with two additional phases. One of the standard way of parametrizing these two ‘‘Majorana phases’’ is

$$V_{(M)} = V \times \text{Diag}[1, e^{i\alpha}, e^{i\beta}] \quad . \quad (62)$$

As can be see from eq. (37), the CP violation in neutrino oscillations in vacuum is proportional to $\text{Im}(U_{\alpha i}^* U_{\beta i} U_{\alpha j} U_{\beta j}^*)$. The unitarity of V ensures that this quantity can only take the values $\pm J$ or 0, irrespective of the flavour eigenstates involved. Here

$$J = s_{12}c_{12}s_{23}c_{23}s_{13}c_{13}^2 \sin \delta \quad , \quad (63)$$

which is known in the quark context as the Jarlskog invariant, determines the extent of observable CP violation in vacuum.

The observation of CP violation is the holy grail of neutrino physics. The matter effects change the values of the mixing matrix elements and can affect the extent of CP violation. It is a formidable task to separate the real CP violation from matter induced CP violation in long baseline neutrino experiments [23].

8 Neutrino mass models

In the standard model, the charged leptons and quarks get their masses through the Yukawa coupling with Higgs. By introducing the right handed counterparts of the left handed neutrinos, the same framework can be naively extended to neutrinos.

However, a few important issues arise while considering the neutrino mass generation. Unlike the other fermions, neutrinos can have Majorana masses. In addition, if right handed neutrinos exist, thus giving neutrinos Dirac masses, they themselves may have large Majorana masses which affect the light neutrino masses through the seesaw mechanism. Moreover, if quark-lepton unification is desired, the drastic difference between the masses and mixing angles in the quark and lepton sector needs to be explained.

8.1 Structure of the neutrino mass matrix

The main properties any neutrino mass model must explain are the small neutrino masses and the hierarchy $\Delta m_{\odot}^2 \ll \Delta m_{atm}^2$, two large mixing angles θ_{12} and θ_{23} , and a small mixing angle θ_{13} . In addition, a model should have predictions regarding whether the mass hierarchy of neutrinos is normal or inverted, whether neutrinos are quasi-degenerate, whether they have Majorana masses, whether there is a significant CP violation, etc..

Given that $\theta_{23} \approx 45^\circ$ and $\theta_{13} \approx 0$, the mixing matrix U should be of the form

$$U = \begin{pmatrix} c_{12} & s_{12} & \theta_{13} \\ -s_{12}/\sqrt{2} & c_{12}/\sqrt{2} & 1/\sqrt{2} \\ s_{12}/\sqrt{2} & -c_{12}/\sqrt{2} & 1/\sqrt{2} \end{pmatrix}, \quad (64)$$

and the mass matrix in the flavour basis would then be

$$M_f = U \begin{pmatrix} m_1 & 0 & 0 \\ 0 & m_2 & 0 \\ 0 & 0 & m_3 \end{pmatrix} U^\dagger, \quad (65)$$

where we have neglected CP violation.

If we neglect Δm_{\odot}^2 , the masses (m_1, m_2, m_3) can be very close to one of the following three forms: $(0, 0, \sqrt{\Delta m_{atm}^2})$ that corresponds to normal hierarchy, $(\sqrt{\Delta m_{atm}^2}, \sqrt{\Delta m_{atm}^2}, 0)$ that corresponds to inverted hierarchy, and (m, m, m) that corresponds to quasi-degenerate neutrinos. In the last case, we have also neglected Δm_{atm}^2 in addition as compared to the mass scale m . There are thus only a few “zeroth order” structures of M_f . These can be further distinguished by their predictions about the effective Majorana mass measured in the neutrinoless double beta decay experiment. The possible structures are tabulated in [24].

Adding Δm^2 corrections and CP violation including the Majorana phases increases the number of possible structures. The important task now is to obtain any of these structures from some fundamental theory. Presumably the structure and the texture (the positioning of zeroes) of the matrix would be a result of some symmetry, e.g. flavour symmetries like $(L_\mu - L_\tau)$. They could be related to the structure of the masses of heavy fermions through a seesaw-like scenario.

8.2 Generating mass from a fundamental theory

An enormous amount of literature exists regarding models of neutrino mass generation from grand unified theories, or by adding new particles that interact with neutrinos giving them masses, and justice cannot be done to them in these notes. In the context of this introductory course, let me just point out a few examples of the models.

- If the neutrino has a Majorana mass at the tree level, it has to be generated through a term $\bar{\nu}_L^c \nu_L X$, where X is a particle. To ensure the gauge invariance of this term, the particle X needs to have electric charge $Q = 0$ and hypercharge $Y = -2$. Therefore, any model that intends to give neutrinos a Majorana mass should predict a particle with these quantum numbers. The simplest such model is the “triplet Higgs” one. The left-right symmetric models also involve triplet Higgses that give masses to neutrinos.
- Neutrinos can get a Majorana mass at the loop level in the models involving “expanded Higgs sector”, where additional singly or doubly charged scalars that couple neutrinos and charged leptons give rise to neutrino masses at one- or two- loop level.
- In the models with grand unified theories, the mechanism of neutrino mass generation depends on the way the symmetry is broken.
- If the neutrino mass comes from its coupling with the SM Higgs, it should come from a term of the form $\bar{X} \Phi \nu_L$. To ensure gauge invariance, X has to be a particle with all SM charges zero. Indeed, the right handed neutrino, which can give a Dirac mass to neutrino, is a SM singlet.

Note that any fermion that is a SM singlet can give rise to a term of this form. This implies that most of the new physics, which involves some SM singlet, in general would affect neutrino masses. The exploration of the origin of neutrino masses can thus be looked upon as the probing of new physics at high scales.

There are also models that involve large extra dimensions of the ADD type where a SM singlet fermion in the bulk gives the neutrinos their mass through such a term. the so-called “volume suppression” that

arises here due to the confining of the SM neutrinos on a 3-brane may account for the smallness of neutrino masses [25].

For a systematic study of various models, the reader is referred to [1, 26].

9 Neutrinos in astrophysics and cosmology

9.1 Supernova neutrinos

Neutrinos play an important role in the SN explosion, and they also carry most of the energy of the collapse. The energy spectra of neutrinos and antineutrinos arriving at the Earth incorporate information on the primary neutrino fluxes as well as the neutrino mixing scenario. The analysis of neutrino propagation through the matter of the supernova and the Earth, combined with the observation of a neutrino burst from a galactic SN, enables us to put limits on the mixing angle θ_{13} and identify whether the mass hierarchy is normal or inverted. The neutrino burst also acts as an early warning signal for the optical observation, and in addition allows us to have a peek at the shock wave while still inside the SN mantle.

For a recent review, please see [27].

9.2 Baryogenesis through leptogenesis

The observed baryon-antibaryon asymmetry in the universe can be generated only when the three Sakharov conditions are satisfied: (1) C and CP violation, (2) B (baryon number) violating interactions, and (3) out of equilibrium conditions. The CP violation in the quark sector of the SM is grossly insufficient to explain the observed value of the baryon asymmetry.

One of the favoured mechanisms for the dynamical generation of the observed baryon asymmetry is through the production of a lepton asymmetry, which can then be converted to the baryon asymmetry by $(B-L)$ conserving electroweak sphalerons [28].

The leptonic asymmetry can be generated, for example, in the CP -violating decay of heavy ($M \sim 10^{10}$ GeV) right handed neutrinos N_i to Higgs and usual neutrinos $N_i \rightarrow \ell^c H^*$, $\ell H \rightarrow N_i$. The lifetime of these Majorana neutrinos needs to be long enough, so that the thermal equilibrium is broken [29].

9.3 Large scale structure, CMBR, etc.

The anisotropies in the cosmic microwave background radiation (CMBR) and observations of the large scale distribution of galaxies probe the primordial density fluctuations in the universe (for scales larger than 100 Mpc). Optical red shift surveys of galaxies can examine scales upto ~ 100 Mpc. These put a limit on the amount of hot dark matter – the particles which were relativistic at $t \sim 1$ year, when $T \sim \text{keV}$ and the “galaxies” came within the horizon. These observations therefore can put an upper bound on the mass of the neutrino. The current most stringent upper bounds on the neutrino masses actually comes from the CMBR observations by WMAP [30].

For a short review of the issues involved in astrophysics and cosmology of neutrinos, please refer to [31]. Note that though the review is only a few years old, some of the things have already become outdated. This exemplifies the rate at which the field is evolving.

10 Current and future experiments

Here is a non-exhaustive list of current and future experiments that study the properties of neutrinos. The websites of these experiments will give more details.

10.1 Neutrino mixing parameters

- Solar neutrino parameters Δm_{\odot}^2 and θ_{12} : SuperKamiokande, KamLAND, KASKA
- Atmospheric neutrino parameters Δm_{atm}^2 and θ_{23} : SuperKamiokande, K2K, MINOS, CNRS
- Measurement of θ_{13} : double CHOOZ, T2K, superbeams, beta beams, NO ν A
- Confirming or ruling out the LSND experiment: miniBOONE
- Normal vs. inverted mass hierarchy: T2K, superbeams, INO (through separation of μ^+ and μ^- in atmospheric neutrinos)
- CP violation: Neutrino factories / muon storage rings

10.2 Origin of neutrino mass

- Dirac vs. Majorana mass: neutrinoless double beta decay at CUORE, MAJORANA, GENIUS, etc.
- Grand unification: proton decay at SK/HK

10.3 Astrophysics and cosmology

- Detection of neutrino burst from a galactic supernova: SK, LVD, HK, LENA, IceCube
- Cosmic microwave background radiation: WMAP, PLANCK
- Ultrahigh energy neutrinos: neutrino telescopes AMANDA, IceCube, ANTARES, NEMO
- Dark matter searches: direct at DAMA, CDMS, indirect through large scale structure at SDSS (Sloan Digital Sky Survey)

11 Final remarks

The field of neutrino physics has emerged as one of the most active, productive and promising areas of research over the past decade. Not only have neutrinos given us the first confirmed signals of physics beyond the standard model (SM) of particle physics, they have also challenged many of our preconceived notions about the nature of mass. They have raised many questions unanswered as yet, and they have also allowed us to take a peek at the fundamental interactions at very high energies that cannot be reached even with particle accelerators. The observations of astrophysical neutrinos that arrive on the Earth from the sun, from the cosmic rays, or from the explosions of supernovae also can be used to extract information about the neutrinos as well as the astrophysical phenomena. The field is buzzing with activity: both theoretical and experimental.

These lecture notes have been an attempt to introduce students to the current excitement in neutrinos. The notes are fairly pedagogical, and clarity has been given more weightage than nitpicking accuracy at a few places. The student is expected to use these as a platform to launch in the field of

neutrinos. For a recent analysis of where the field is and where it is going, please refer to [32].

References

- [1] R. N. Mohapatra and P. B. Pal, “Massive neutrinos in physics and astrophysics. Second edition,” World Sci. Lect. Notes Phys. **60** (1998) 1.
- [2] C. W. Kim and A. Pevsner, “Neutrinos in physics and astrophysics,” Harwood Academic Publishers, 1993.
- [3] E. K. Akhmedov, “News about nu’s,” hep-ph/0011353.
- [4] S. Eidelman et al [Particle data Group], Phys. Lett. B **592** (2004) 1.
- [5] G. Danby et al, “Observation Of High-Energy Neutrino Reactions And The Existence Of Two Kinds Of Neutrinos,” Phys. Rev. Lett. **9** (1962) 36.
- [6] K. Kodama *et al.* [DONUT Collaboration], “Observation of tau-neutrino interactions,” Phys. Lett. B **504** (2001) 218 [hep-ex/0012035].
- [7] T. D. Lee and C. N. Yang, “Question Of Parity Conservation In Weak Interactions,” Phys. Rev. **104** (1956) 254.
- [8] C. S. Wu, E. Ambler, R. W. Hayward, D. D. Hoppes and R. P. Hudson, “Experimental Test Of Parity Conservation In Beta Decay,” Phys. Rev. **105** (1957) 1413.
- [9] J. I. Friedman and V. L. Telegdi, “Nuclear Emulsion Evidence For Parity Nonconservation In The Decay Chain $\text{Pi}^+ \text{Mu}^+ \text{E}^+$,” Phys. Rev. **105** (1957) 1681.
- [10] Y. Ashie et. al. [Super-Kamiokande Collaboration], “A Measurement of Atmospheric Neutrino Oscillation Parameters by Super-Kamiokande I,” hep-ex/0501064.
- [11] L. Wolfenstein, “Neutrino Oscillations In Matter,” Phys. Rev. D **17** (1978) 2369.

- [12] S. P. Mikheev and A. Y. Smirnov, “Resonance Enhancement Of Oscillations In Matter And Solar Neutrino Spectroscopy,” *Sov. J. Nucl. Phys.* **42** (1985) 913 [*Yad. Fiz.* **42** (1985) 1441].
- [13] M. Kachelrieß and R. Tomas, “Non-adiabatic level crossing in (non-) resonant neutrino oscillations,” *Phys. Rev. D* **64** (2001) 073002 [hep-ph/0104021].
- [14] T. K. Kuo and J. T. Pantaleone, “Nonadiabatic Neutrino Oscillations In Matter,” *Phys. Rev. D* **39** (1989) 1930.
- [15] A. S. Dighe, Q. Y. Liu and A. Y. Smirnov, “Coherence and the day-night asymmetry in the solar neutrino flux,” hep-ph/9903329.
- [16] J. N. Bahcall, “Solar models and solar neutrinos: Current status,” hep-ph/0412068.
- [17] J. N. Bahcall and A. M. Serenelli, “New solar opacities, abundances, helioseismology, and neutrino fluxes,” astro-ph/0412440.
- [18] H. Back *et al.*, “Report of the solar and atmospheric neutrino experiments working group of the APS multidivisional neutrino study,” hep-ex/0412016.
- [19] S. Goswami, A. Bandyopadhyay and S. Choubey, “Global analysis of neutrino oscillation,” hep-ph/0409224.
- [20] M. Apollonio *et al.* [CHOOZ Collaboration], “Limits on neutrino oscillations from the CHOOZ experiment,” *Phys. Lett. B* **466** (1999) 415 [hep-ex/9907037].
- [21] A. Aguilar *et al.* [LSND Collaboration], “Evidence for neutrino oscillations from the observation of anti- ν /e appearance in a anti- ν / μ beam,” *Phys. Rev. D* **64** (2001) 112007 [hep-ex/0104049].
- [22] C. Aalseth *et al.*, “Neutrinoless double beta decay and direct searches for neutrino mass,” hep-ph/0412300.
- [23] P. Huber, M. Lindner and W. Winter, “From parameter space constraints to the precision determination of the leptonic Dirac CP phase,” hep-ph/0412199.

- [24] S. F. King, “Neutrino mass models,” Rept. Prog. Phys. **67** (2004) 107 [hep-ph/0310204].
- [25] K. R. Dienes, E. Dudas and T. Gherghetta, “Light neutrinos without heavy mass scales: A higher-dimensional seesaw mechanism,” Nucl. Phys. B **557** (1999) 25 [hep-ph/9811428].
- [26] A. Y. Smirnov, “Neutrino physics: Open theoretical questions,” Int. J. Mod. Phys. A **19** (2004) 1180 [hep-ph/0311259].
- [27] A. Dighe, “Supernova neutrinos: Production, propagation and oscillations,” hep-ph/0409268.
- [28] M. Fukugita and T. Yanagida, “Baryogenesis Without Grand Unification,” Phys. Lett. B **174** (1986) 45.
- [29] W. Buchmuller, P. Di Bari and M. Plumacher, “Leptogenesis for pedestrians,” hep-ph/0401240.
- [30] D. N. Spergel *et al.* [WMAP Collaboration], “First Year Wilkinson Microwave Anisotropy Probe (WMAP) Observations: Determination of Cosmological Parameters,” Astrophys. J. Suppl. **148** (2003) 175 [astro-ph/0302209].
- [31] A. Dighe, S. Pastor and A. Smirnov, “The physics of relic neutrinos,” hep-ph/9812244.
- [32] R. N. Mohapatra *et al.*, “Theory of neutrinos,” hep-ph/0412099.